ISSN (Print) 1226-1750
ISSN (Online) 2233-6656
Journal of Magnetics 23(2), 171-178 (2018) https://doi.org/10.4283/JMAG.2018.23.2.171

Design and Simulation of the Channel Model of a LMMHD Generator Based on Halbach

Xinyue Feng*, Yiming Zhang, Jiashen Tian, and Junxia Gao

Faculty of Information Technology, Beijing University of Technology, 100 Ping Le Yuan, Chaoyang District, Beijing 100124, China

(Received 25 December 2017, Received in final form 14 May 2018, Accepted 15 May 2018)

To improve the efficiency of the liquid metal magnetohydrodynamic (LMMHD) generator, a new type of magnet structure of LMMHD system is designed in paper. The internal magnetic gathering capability is enhanced by imitating the arrangement of the Halbach array magnet. The magnetic induction intensity of conventional magnetic channel, Halbach magnet channel, and the new type of magnet channel, which is derived from basic Halbach are compared via ANSYS Maxwell 2D model. Simulation results show that Halbach magnets have better capacity of magnetism gathering and are more efficient at gathering electricity than conventional methods. The new type of magnetic has advantages of small size, low cost, high induction intensity, high output voltage and high power.

Keywords : liquid metal magnetohydrodynamic (LMMHD), magnetoelectric channel, Halbach, ocean power generation, power generation efficiency

1. Introduction

The LMMHD power generation system uses wave energy as the driving force and adopts a reciprocating LMMHD generator, whose speed-torque characteristics excellently match the mechanical impedance of an ocean wave, thus avoiding an intermediate step [1-3]. In traditional wave power generation systems, a series of energy conversion and transmission devices are adopted. In recent years, the use of a liquid metal as the medium wave energy power magnetohydrodynamic (MHD) generator is proposed [4, 5]. This is able to use huge force of wave, direct drive high speed liquid metal of high conductivity, which flow through the channel, cut magnetic lines, and generate electricity. This method of power generation not only improves the efficiency and reliability of the system and reduces cost, but also has advantages of compact structure, simple installation, and free maintenance [6, 7].

To improve power generation efficiency, a great deal of recent research has focused on the design of magnetiofluid channel and the finite element method of magnetic field sealing structure of the magnetic field in the magnetic circuit design [8, 9]. In the practical MHD device, certain effects cause degradation of the performance and the end effect is one of them. Ohmic losses are evaluated in a MHD channel with large magnetic Reynolds number [10, 11]. The influence of the induced magnetic field on the LMMHD generator is studied by Satake and Maeda [12]. The results show that as the induced magnetic field increases with the inlet velocity of liquid metal, the generator performance decreases. The magneto hydrodynamic flow in the LMMHD generator performance is analyzed via 2-D and 3-D numerical analyses. Lin and Peng suggest using a tapered magnetic field and a tapered flow channel outside electrodes can effectively reduce the end loss [13]. Kim numerically examined three-dimensional LMMHD flows in a rectangular duct with sudden expansion. Computational fluid dynamics simulations are performed to predict the behavior of the MHD flows in the duct [14-16]. A three-dimensional simulation for a LMMHD duct flow is performed numerically by Mao and Pan [17]. However, the magnet design of the LMMHD generator channel outside is rarely studied and reported. As one of the most important components of the MHD generator, the magnet is designed by Xu. Detailed simulation, optimization and calculation results of the magnet manufacturing have played a very important role in the guidance of the development [18].

*Corresponding author: Tel: 010-67392391
Fax: 010-67391625, e-mail: 739671532@qq.com

Underwater battery life is limited, and liquid metal can be used to cut the magnetic flux lines through the advance of seawater, which can generate electricity. The purpose of this paper is to reconstruct the magnet structure based on a Halbach array magnet, which improves the internal magnetic gathering capability. In addition, the utilization rate of magnets and the power generation efficiency are discussed. The magnet volume is smaller than conventional cases, and internal magnetic induction intensity probably increases two-fold. Furthermore, ferrite magnetic material is added to both ends of the magnet, increasing the internal magnetic induction about three-fold. This design not only shortens the intermediate mechanical energy conversion processes, but also improves the utilization rate of the magnets and the power generation efficiency.

2. Design of Halbach Array Permanent Magnet for LMMHD Generator

A conventional LMMHD generator consists of a magnet, an electrode, a power path, and a liquid metal. Fig. 1 shows the model of permanent magnets of conventional LMMHD generator. In Fig. 1, a_1 and d_1 are the channel width and height of a conventional LMMHD generator. b_1 and L_1 are the width and length of each magnet. c_1 is the height of the LMMHD generator. The principle of power generation is shown in Fig. 2, where B, v and R_L represent the magnetic induction, flow velocity and the resistance load. Liquid metal cuts magnetic induction lines in a magnetic field, and generates an induced electromotive force. The electrode is connected to an external load, which provides electrical energy.

B is in z direction, v is in y direction, and the electromagnetic field and the flow field are evenly distributed

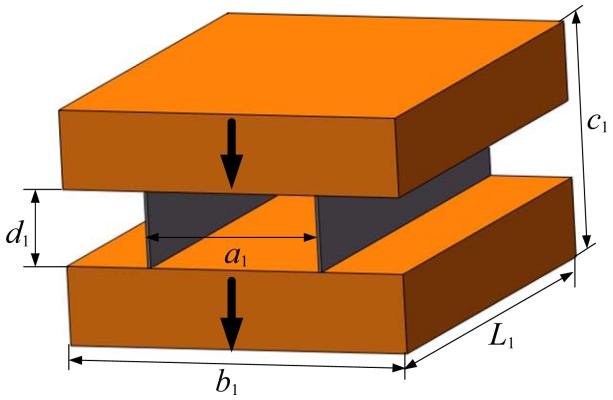

Fig. 1. (Color online) Model of permanent magnets of conventional magnetofluid channel.

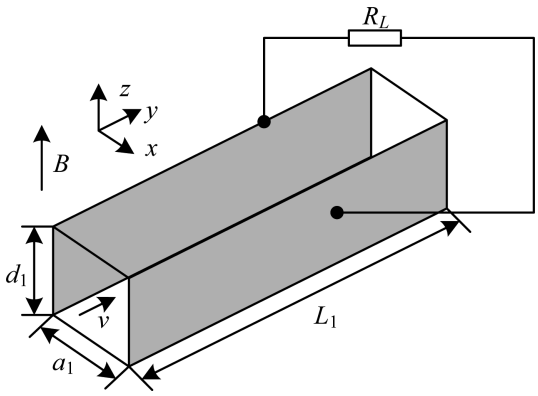

Fig. 2. Conventional magnetofluid generator magnet model.

without considering the induced magnetic field. After connecting the resistance load R_L, steady-state electromagnetic parameters are as follows.

According to Electromagnetic Induction Law, the electromotive force of the conventional LMMHD generator can be calculated as:

$$E = Ba_1v \tag{1}$$

From (1), the short-circuit current can be expressed as follow:

$$I_{\max} = \frac{Ba_1v}{R_g} \tag{2}$$

where R_g is the internal resistance of the generator, which can be calculated as follow:

$$R_g = \frac{a_1}{d_1L_1\sigma} \tag{3}$$

where σ is the conductivity of liquid metal.

Define

$$K = \frac{R_L}{R_L + R_g} \tag{4}$$

From (1) and (4), the load voltage can be expressed as:

$$U_L = KBa_1v \tag{5}$$

Then, the load current can be expressed as:

$$I_L = \frac{KBa_1v}{R_L} \tag{6}$$

Combining (4), (5) and (6), the output power of the generator can be calculated as:

$$P_L = B^2v^2\frac{R_L}{(R_L + R_g)^2}a^2 \tag{7}$$

The input power of the generator is given by:

$$P_0 = \Delta p v a_1 d_1 \tag{8}$$

where Δp is the static pressure difference between inlet and outlet.

Therefore, the generator efficiency can be calculated as follow:

$$\eta = \frac{P_L}{P_0} \tag{9}$$

The utilization rate of the magnets can be defined as:

$$\eta_0 = \frac{B}{V} \tag{10}$$

where V is the volume of the magnets.

The Halbach array permanent magnet has good self-shielding effect, and can produce a static magnetic field, which is larger than the residual magnetic field strength, and has a wide application prospect [19, 20]. By changing the magnetic circuit, it can collect magnetic flux, enhance the magnetic density of one side, weaken the flux density on the other side, and realize the maximization of magnet utilization. The use of Halbach arrays in LMMHD generators reduces the consumption of permanent magnets. This new array can produce higher power density than conventional radial arrays, thus greatly reducing the volume of the magnets. Fig. 3 is a square magnetofluid channel based on a Halbach array.

The high altitude of the Halbach channel, affects the volume of the magnet. Based on the size of normal magnetiofluid channel, this paper designs a new type of magnetiofluid power channel based on Halbach. The model is shown in Fig. 4.

To keep the volume of the magnets as consistent as possible, the magnetic body size of the three magnetiofluid power channels is shown in the following Table 1.

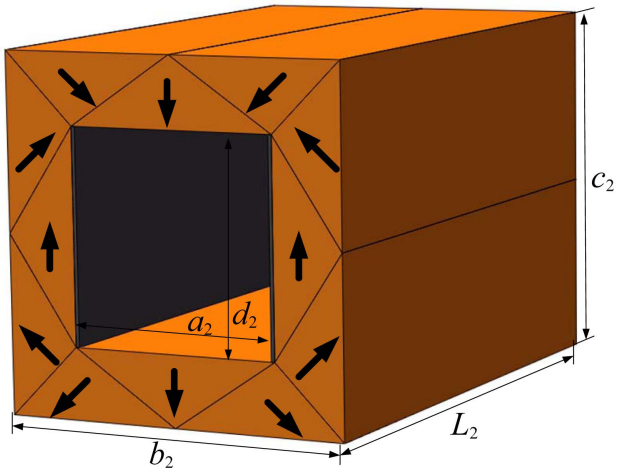

Fig. 3. (Color online) Square magnetofluid channel based on Halbach array.

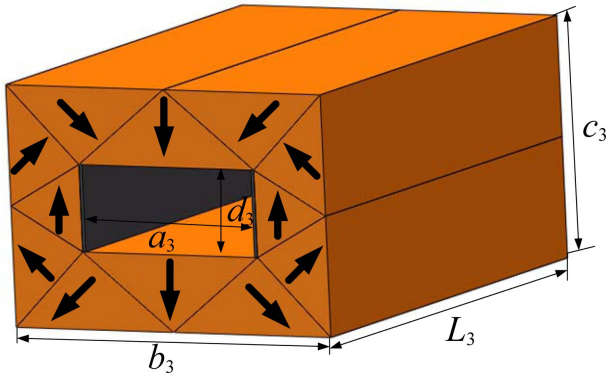

Fig. 4. (Color online) New type of magnetiofluid power channel based on Halbach.

Table 1. The size of magnetofluid power channel parameters.

Parameters	Values
Width of channel (a_1)	60 mm
Width of channel (a_2)	60 mm
Width of channel (a_3)	60 mm
Width of magnet (b_1)	120 mm
Width of magnet (b_2)	100 mm
Width of magnet (b_3)	108 mm
Length (L_1)	160 mm
Length (L_2)	160 mm
Length (L_3)	160 mm
Height of channel (d_1)	27 mm
Height of channel (d_2)	60 mm
Height of channel (d_3)	27 mm
Height of generator (c_1)	81 mm
Height of generator (c_2)	100 mm
Height of generator (c_3)	75 mm

According to table 1, the volume of the magnetic body of the normal channel is 1036800 mm^3, which can be calculated by

$$V_1 = b_1 L_1 \left(\frac{c_1 - d_1}{2} \right) \tag{10}$$

The volume of the magnetiofluid power channel based on Halbach is 1024000 mm^3, which can be calculated by

$$V_2 = b_2 L_2 c_2 - a_2 L_2 d_2 \tag{11}$$

The volume of the new magnetiofluid power channel is 1036800 mm^3, which can be calculated by

$$V_3 = b_3 L_3 c_3 - a_3 L_3 d_3 \tag{12}$$

3. The two-Dimensional Field Solution of the Ideal Halbach Array

The Halbach array magnet structure is an approximate ideal structure, and the goal is to generate the strongest magnetic field with the least weight of magnetics [21-23]. In a vacuum, the two dimensional magnetic field components B_x, and B_y can be obtained either by scalar magnetic bits V or by vector magnetic bits A:

$$B_x = \partial A/\partial y = -\partial V/\partial x \tag{10}$$

$$B_y = -\partial A/\partial x = \partial V/\partial y \tag{11}$$

The relationships between the vector magnetic bit A and the scalar magnetic bit V is the same as the Cauchy Riemann conditions of the real and imaginary part of complex variable z, which means that the complex vector $\vec{F}$ can be expressed as:

$$\vec{F} = A + jV \tag{12}$$

The two-dimensional field vector is expressed as:

$$\vec{B} = B_x + jB_y \tag{13}$$

The relationship can be expressed as:

$$\overrightarrow{B^*} = jd\vec{F}/d\vec{z} \tag{14}$$

Among them $\overrightarrow{B^*}$ represents the conjugate complex of $\vec{B}$.

To facilitate the analysis of the subharmonic components in the static magnetic field, $\vec{F}$ and $\overrightarrow{B^*}$ can be unfolded as a Taylor series, which is in the point $\vec{z_0}$:

$$\vec{F}(\vec{z_0}) = \sum \vec{a_k}\vec{z_0^k} \tag{15}$$

According to the equation 14:

$$\overrightarrow{B^*}(\vec{z_0}) = \sum_{k=1} \vec{b_k}\vec{z_0^k} \tag{16}$$

Among them $\vec{b_k} = jk\vec{a_k}$.

Equation (15) and (16) can be used to describe the magnetic field inside the array magnet, when k = 1, 2, 3 … and describe the magnetic field outside the array magnet, when k = –1, –2, –3 …

According to the classical electromagnetic field theory, in the absence of ferromagnetic materials, the magnetic field of any point $\vec{z_0}$ outside the magnet can be expressed as a magnetic field generated by the current density J, which is located in the $\vec{z_0}$:

$$\overrightarrow{B^*}(\vec{z_0}) = \frac{1}{2\pi}\iint \frac{\vec{B_r}}{(\vec{z_0} - \vec{z})^2} dxdy \tag{17}$$

Among them, $\vec{B_r} = B_{rx} + jB_{ry}$ is the vector with the magnitude of the remanent field and in line with the direction of magnetization.

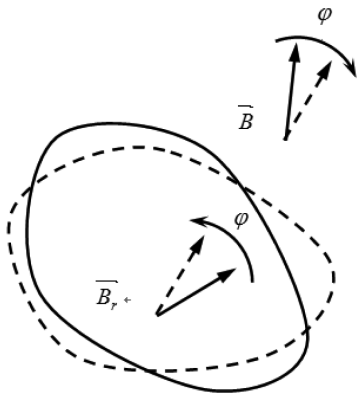

Fig. 5. Easy Axis Rotation theorem.

Since rare earth permanent magnets can be considered as a collection of many individual volume elements, each volume element generates a dipole magnetic field. If every element of $+\varphi$ rotating direction of magnetization is relative to the original position, it is on the right side of equation (17) multiplied $e^{j\varphi}$. This explains the "Easy Axis Rotation Theorem", which indicates that in the two-dimensional space without the magnetic material, the magnetization direction of all the rare earth magnets is rotated $+\varphi$, and the magnetic fields in space rotate $-\varphi$. However, the amplitude does not change.

For rare earth permanent magnets, which are the uniform magnetization, the residual magnetism $\vec{B_r}$ can be presented from the integral number of the equation (17).

If x is integrated first, equation (17) can be expressed as:

$$\overrightarrow{B^*}(\vec{z_0}) = \frac{\vec{B_r}}{2\pi} \bullet \oint \frac{dy}{\vec{z_0} - \vec{z}} \tag{18}$$

If y is integrated first, the equation can be expressed as:

$$\overrightarrow{B^*}(\vec{z_0}) = -\frac{\vec{B_r}}{2\pi j} \bullet \oint \frac{dx}{\vec{z_0} - \vec{z}} \tag{19}$$

Because $\vec{z} = x + jy$, combining (18) and (19), the equation (17) can also be expressed as:

$$\overrightarrow{B^*}(\vec{z_0}) = -\frac{\vec{B_r}}{4\pi j} \bullet \oint \frac{d\vec{z}^*}{\vec{z_0} - \vec{z}} \tag{20}$$

According to the geometrical shape of permanent magnet material, equations (18) to (20) can be used to solve the two-dimensional magnetic field. For a more convenient understanding of the essential characteristics of the two-dimensional magnetic field, equations (18) to (20) can be extended to a Taylor series form.

To obtain the corresponding expansion coefficient:

$$\frac{1}{\vec{z_0}-\vec{z}} = -\sum_{k=1}^{\infty} \frac{\overrightarrow{z_0^{k-1}}}{\vec{z^k}} \tag{21}$$

If it is the form of equation (17), equation (21) can be differentiated by $\vec{z}$:

$$\frac{1}{(\vec{z_0}-\vec{z})^2} = \sum_{k=1}^{\infty} \frac{k\overrightarrow{z_0^{k-1}}}{\overrightarrow{z^{k+1}}} \tag{22}$$

For the magnetic field distributed outside the array, it can be expressed as:

$$\frac{1}{\vec{z_0}-\vec{z}} = \sum_{k=-1}^{-\infty} \frac{\overrightarrow{z_0^{k-1}}}{\vec{z^k}} \tag{23}$$

$$\frac{1}{(\vec{z_0}-\vec{z})^2} = -\sum_{k=-1}^{-\infty} \frac{k\overrightarrow{z_0^{k-1}}}{\overrightarrow{z^{k+1}}} \tag{24}$$

Equation (22) can be plugged into equation (17) and compared with equation (16):

$$\vec{b_k} = \frac{k}{2\pi} \iint \frac{\vec{B_r}}{\overrightarrow{z^{k+1}}} dxdy \tag{25}$$

To construct a strong multipole magnet with good field quality, equation (16) should be guaranteed to be as large as possible, while the other should be as small as possible.

$$\vec{B_r} = B_r e^{j\beta(\varphi)} \tag{26}$$

Bring equation (26) with equation $\vec{z} = re^{j\varphi}$ in equation (25):

$$\vec{b_k} = \frac{k}{2\pi} \int \frac{B_r \exp\left(j(\beta(\varphi)-(k+1)\bullet\varphi)\right)}{r^{k+1}} rdrd\varphi \tag{27}$$

Assuming the function of the magnetized vector of the permanent magnet is as follows, the schematic diagram is shown in Fig. 6:

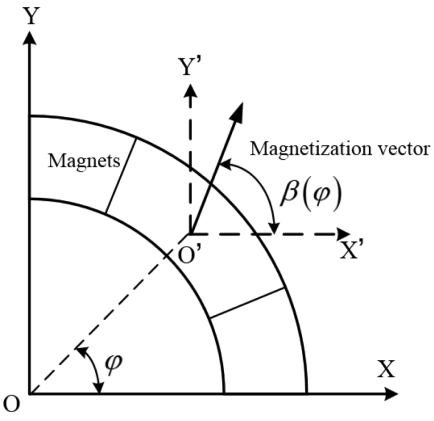

Fig. 6. Magnetization of Halbach array.

For the value of $\vec{b_k}$ to be able to obtain the largest real number possible, the direction of the magnetized vector in type (27) should be taken as:

$$\beta(\varphi) = (N+1)\bullet\varphi \tag{28}$$

where φ is the angular position of the magnetization direction in one segment, $\beta(\varphi)$ is the magnetization angular, N is the polar logarithm of the magnetic field. In theory, the magnetization direction of a segment with the angular position φ must be 2φ to model the ideal dipole field.

If the Halbach array is filled with B_r constant rare earth permanent magnet material and the magnetization direction is determined by equation (28), the magnetic induction intensity in the Halbach array is:

$$\vec{B^*}(\vec{z_0}) = \left(\frac{\vec{z_0}}{r_i}\right)^{N-1} B_r \frac{N}{N-1}\left(1-\left(\frac{r_i}{r_0}\right)^{N-1}\right) \quad N \geq 2 \tag{29}$$

$$\vec{B^*}(\vec{z_0}) = B_r \ln\left(\frac{r_0}{r_i}\right) \quad N = 1 \tag{30}$$

It can be seen that when the number of pole-pairs N=1, the structure is ideal for a single pair of polar (bipolar) Halbach arrays. Equation (30) can be seen that the internal magnetic induction intensity is equal to a certain value, and the amplitude value is only affected by the diameter ratio of the array. When a suitable thickness of magnet is obtained, the magnetic induction intensity of the magnetic field can exceed the residual magnetic value of the permanent magnet material itself.

Because of this advantage of the Halbach array magnet, this paper designs a new type of magnetiofluid generation channel. The magnetic field in all space is provided by the magnetomotive in the magnetic field, and the increase in space utilization reduces the required magnetomotive, which is the saving of magnetic materials. This is the theoretical basis of using the Halbach array magnet to reduce the cost of the generator magnet, reduce its volume, and reduce its weight.

4. Compare and Analyze Simulation Results

In this paper, Ansoft is used to simulate the finite element simulation. The magnetic induction intensity is not uniform in the conventional magnetoelectric channel, whose length is 60 mm. The black arrow is the direction of the magnetization. As shown in Fig. 7 and Fig. 8, at the center, the magnetic induction line is vertically downward and the magnetic induction intensity is 0.24 T.

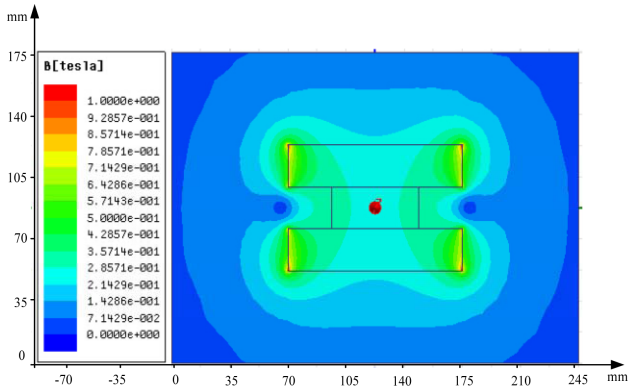

Fig. 7. (Color online) Magnetic induction intensity in conventional magnets.

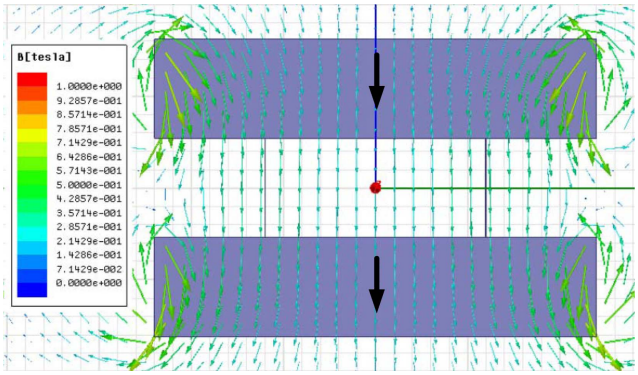

Fig. 8. (Color online) The distribution of magnetic induction lines in conventional magnets.

However, the magnetic induction line on both sides is curved to the sides and the magnetic induction intensity is 0.29 T.

Figure 9 shows the magnetic flux density distribution of the outer space of the Halbach array to have zero magnetic induction intensity, and the internal magnetic induction intensity is 0.54 T. Figure 10 shows that all

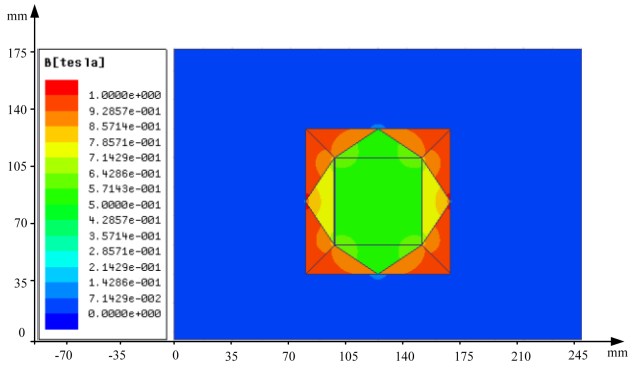

Fig. 9. (Color online) Magnetic induction intensity of the magnetic array based on Halbach.

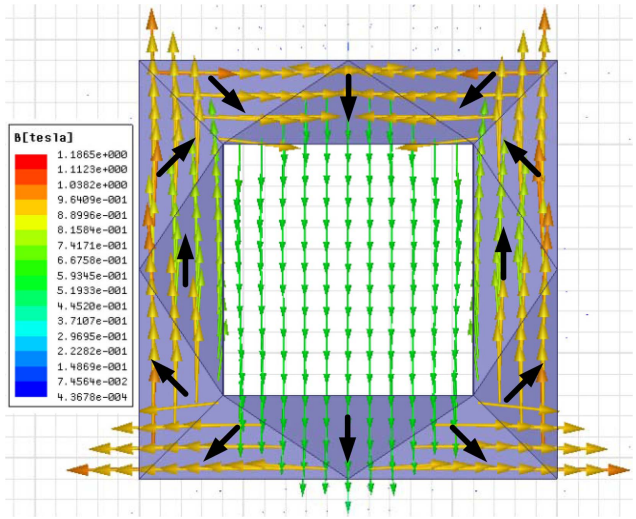

Fig. 10. (Color online) Distribution of magnetic flux lines in the magnetic array based on Halbach.

magnetic flux is closed through the permanent and internal air gap, and the utilization rate of permanent magnet materials is extremely high. Therefore, this compact self-shielded Halbach array magnet is ideal for the static magnetic field of magnetohydroelectric equipment.

Figure 11 shows the transformed new magnetiofluid generation channel, in which the magnetic induction intensity is 0.85 T. In the same volume of magnets, the magnetic induction intensity generated in the new magnetiofluid power generation channel is stronger than that of the magnetiofluid generation channel based on Halbach. As shown in Fig. 12, the magnetic flux line inside the magnetiofluid power channel is vertically downward and the magnetic path is closed. Therefore, the design of this new magnetiofluid power channel enhances the internal magnetic induction intensity B, almost threefold. Then, both output voltage and power generation are improved.

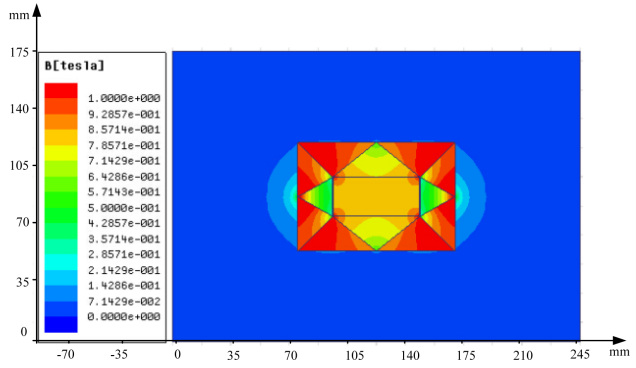

Fig. 11. (Color online) Magnetic induction intensity of the transformed magnetoelectric channel.

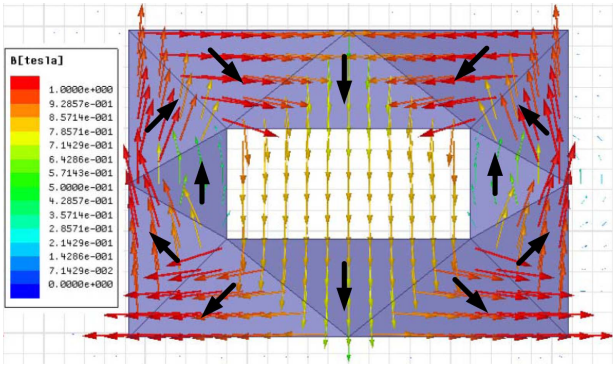

Fig. 12. (Color online) Distribution of magnetic flux lines in the transformed magnetoelectric channel.

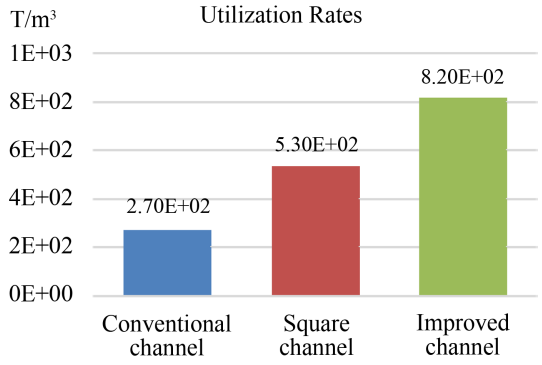

Fig. 13. (Color online) Utilization rate comparison of three magnetiofluid power channels.

Since the power channel design of the simulation result shows that the Halbach array magnets based on each magnet magnetization direction differs, which can lead to an external magnetic flux of zero. All magnetic flux is closed through the permanent magnet, and the utilization rate of the permanent magnet material is very high.

Table 2 presents the volume V of three types of magnetiofluid power generation channels, magnetic induction strength B, induced voltage E, and output power P. Appropriately increasing the length of the power generation channel and increasing the volume of the magnetic body of the power generation channel will increase power generation. It can be seen from the table that in the case of the Halbach array, magnet volume below the normal volume, the magnetic induction intensity of Halbach array is nearly twice as high as that of conventional magnets. The induction voltage E and output power P are improved correspondingly. The transformed new magnetiofluid power generation channel, which fully utilizes the permanent magnet, has the strongest internal magnetic induction and the most efficient power generation.

From equation (8), (9) and Table 2, it can be concluded that the efficiency of the proposed generator channel (shown in Fig. 4) is 7.54 times larger than that of the conventional generator channel (shown in Fig. 1).

From equation (10) and Table 2, the utilization rate of three kinds of magnets is compared in Fig. 13. It can be seen that the proposed generator channel has improved the utilization rate significantly.

In the case of the length of the generator channel and the same velocity of liquid metal, there is greater magnetic induction intensity B, the higher the power generation efficiency. Therefore, it is very significant to design the power channel magnet. Figure 14 shows the

Table 2. Contrast the model of different magnetiofluid generation channels.

Items	Conventional	Halbach	Transformed
V ($\times 10^{-3}$ m^3)	1.0368	1.024	1.0368
B (T)	0.29	0.54	0.85
E (V)	0.034	0.065	0.097
P (W)	199	700	1500

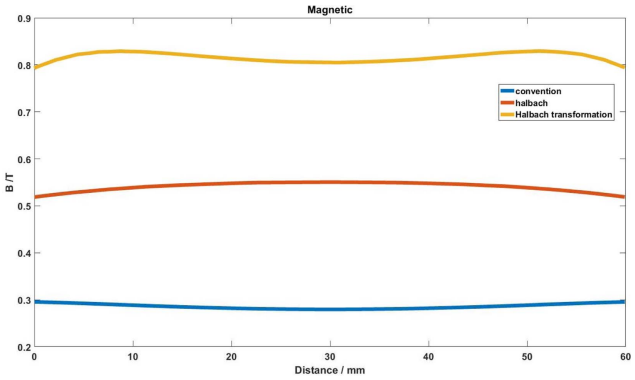

Fig. 14. (Color online) Magnetic induction intensity B constrast curve of three magnetiofluid power channels.

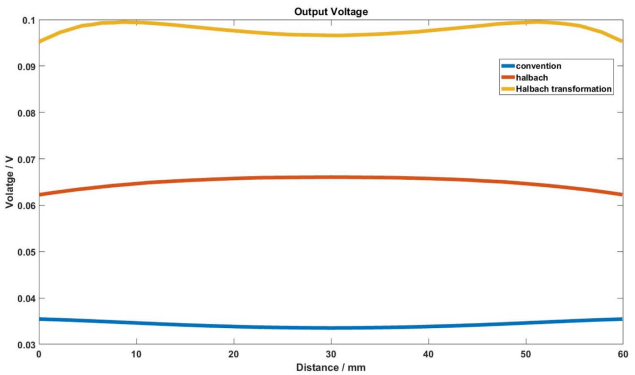

Fig. 15. (Color online) Internal induction voltage contrast curve of three kinds of magnetiofluid power generation channels.

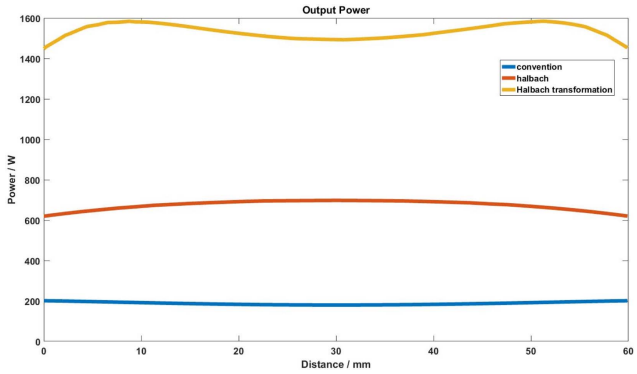

Fig. 16. (Color online) Power comparison curves of three types of magnetiofluid power generation channels.

improved magnet channel generates the largest magnetic induction intensity and the highest utilization of magnets. As can be seen from Fig. 15, the output voltage of the new liquid magnetiofluid power generation channel is the largest, with the highest efficiency in the same external conditions. The velocity of liquid metal in a magnetiofluid generator is 600-1000 m/s, and the generation power is shown in Fig. 16, which is obviously the most efficient of the new type of magnetiofluid generator.

5. Conclusions

To conclude, the transformed magnetoelectric channel magnet model, which is suitable for liquid metal magnetiofluid generators with the higher induced voltage and the higher output power, has been proposed in this paper. The theoretical calculation of Halbach array magnet shows that the model of channel, which is transformed based on Halbach, causes an equal internal magnetic induction intensity, and the magnetic induction intensity of the external magnetic field is zero. Through comparison with conventional power channel, the improved new magnetiofluid power channel magnet model enables all magnetic flux to be closed through the permanent magnet and internal air gap, and the utilization rate of permanent magnet material is extremely high. Therefore, this compact self-shielded Halbach array magnet, which is transformed, is ideal for the static magnetic field of magnetohydroelectric equipment.

Acknowledgement

This work was supported by the strategic pilot science and technology project of the Chinese academy of sciences (research on key technology of marine electromagnetic launch equipment of controllable source in sea bucket deep area) under; grant No. XDB06030204.

References

[1] P. Lu, X. Zheng, and H. Huang, Ind. Eng. Chem. Res. **56**, 35 (2017).
[2] P. Satyamurthy, T. K. Thiyagarajan, and N. Venkatramani, Energ. Convers. and Manage. **36**, 10 (1995).
[3] J. Y. Shang and C. N. Kim, Fusion Eng. Des. **121** (2017).
[4] P. Lu, X. W. Zheng, P. J. Yang, L. L. Fang, and H. L. Huang, RSC Advances **7**, 57 (2017).
[5] L. Hu, H. Kobayashi, and Y. Okuno, IEEJ Trans. on Power and Energy. **134**, 12 (2014).
[6] B. L. Liu, J. Li, Y. Peng, L. Z. Zhao, R. Li, Q. Xia, and C. W. Sha, J. Ocean and Wind Energy **2**, 1 (2015).
[7] Z. Wang, Y. G. Li, S. M. Wang, Q. Y. He, and J. Zhang, Applied Mech. and Mater. Trans. Tech. Publications. 556 (2014).
[8] X. L. Yang, D. C. Li, W. M. Yang, F. F. Xing, and Q. Li, J. Vac. Sci. Technol. **32**, 10 (2012).
[9] M. Zhao, J. B. Zou, and J. H. Hu, J. Magn. Magn. Mater. 303 (2006).
[10] R. Thiele and H. Anglart. Nucl. Eng. Des. **254** (2013).
[11] M. Dupocheel, et al., Int. J. Heat Mass. Tran. **75** (2014).
[12] S. Satake, T. Maeda, K. Shimizu, T. Fujino, and M. Ishikawa, AIAA lasmadynamics and Lasers Conf. (2007).
[13] Z. W. Lin, Y. Peng, L. Z. Zhao, C. W. Sha, Y. Y. Xu, R. Li, and J. Jia, AIAA Plasmadynamics and Lasers Conf. (2007).
[14] C. N. Kim, J. Mech. Sci. Technol. **28**, 12 (2014).
[15] C. N. Kim, Comput. Fluids. **108** (2015).
[16] C. N. Kim, Fusion Sci. Technol. **64**, 4 (2013).
[17] J. Mao and H. Pan, Fusion Eng. Des. **88** (2013).
[18] Y. Y. Xu, Y. Peng, L. Z. Zhao, R. Li, B. L. Liu, J. Li, C. W. Sha, and W. D. Wei, Proceedings of the third academic symposium of the China renewable energy institute of China (2010).
[19] M. Bocian, J. Kaleta, D. Lewandowski, and M. Przybylski, J. Magn. Magn. Mater. 435 (2017).
[20] R. Teyber, P. V. Trevizoli, T. V. Christiaanse, P. Govindappa, I. Niknia, and A. Rowe, J. Magn. Magn. Mater. 442 (2017).
[21] C. W. Kim and J. Y. Choi, J. Magn. **21**, 1 (2016).
[22] J. You, K. Zhang, Z. W. Zhu, and H. Liang, J. Magn. **21**, 1 (2016).
[23] H. M. C. Beigi and S. Akbari, J. Magn. **20**, 4 (2015).